Dual Fluorescence of 9-(*N*,*N*-Dimethylamino)anthracene: Effect of Solvent Polarity and Viscosity

Joykrishna Dey and Isiah M. Warner*

Department of Chemistry, Louisiana State University, Baton Rouge, Louisiana 70803

Received: November 20, 1996; In Final Form: May 2, 1997[⊗]

Absorption and fluorescence spectra of 9-(*N*,*N*-dimethylamino)anthracene (9-DMA) have been studied in a series of organic solvents and water. The induced circular dichroic spectra of 9-DMA were measured in β- and γ-cyclodextrins to locate the position of the ^1L_a and ^1L_b transitions in the absorption spectrum. The fluorescence spectra of 9-DMA exhibit dual emission bands in the solvents employed. Absorption and fluorescence excitation spectra of 9-DMA exhibit a local and an underlying charge-transfer band. The effects of temperature, solvent polarity, and viscosity on these spectra have been studied. The steady-state fluorescence polarization spectra were used to examine the transitions involved. The fluorescence quantum yields and lifetimes of 9-DMA in neat solvents and solvent mixtures have been measured. The pK_a value of nitrogen protonation was estimated in aqueous solution. Semiempirical AM1 calculations were performed to calculate energies and dipole moments of various conformers of 9-DMA obtained by twisting the $-N(CH_3)_2$ group around the C−N bond.

Introduction

Dual fluorescence from organic molecules is the result of a variety of phenomena. For example, dimers and other small molecular aggregates, molecular exciton, excimer, and charge-transfer complexes can give rise to dual emission in solution. The most frequently studied types of dual fluorescence involve a twisted intramolecular charge transfer (TICT) state emission[1−4] and an excited-state intramolecular proton transfer (ESIPT).[5,6] The TICT model was first suggested by Rotkiewicz and Grabowski[2,3] to account for the large Stokes shifted emission of *p*-(*N*,*N*-dimethylamino)benzonitrile (DMABN) in polar solvents. This model clearly demonstrates that the anomalous long-wavelength fluorescence (F_a) of this molecule is due to a state with a strong charge-transfer (CT) character. This CT character is caused by a twisted conformation that the molecule acquires in the TICT state. The idea of a TICT state is based on a principle that associates minimum orbital overlap with intramolecular charge separation.[3,7]

The TICT phenomena has been extended to other structurally related molecules with abnormal dual fluorescence.[8] These molecules often have an aromatic structure with an acceptor and donor group at the para positions. The donor group is usually a dialkylamine, $N(R)_2$, and the acceptor groups are −CN, −CHO, −COOH, −COOR, and $-SONH_2$. However, aromatic structures that can bend about a single bond, such as bianthryl[9], *p*-(9-anthryl)-*N*,*N*-dimethylaniline (ADMA),[10] 2-(4′-(*N*,*N*-dimethylamino)phenyl)benzimidazole, and benzothiazole[11] are also reported to act as either donor or acceptor groups. The para-substituted *N*,*N*-dialkylanilines that are flat in the ground state make a complete twist in the excited state. In addition, molecules such as 4-cyano-*N*,*N*-2,6-tetramethylaniline (CTMA), which are already twisted at an angle of 60° in the ground state, are also known to exhibit anomalous fluorescence.[12] These molecules complete their twist in the excited state before emitting. Most researchers, however, have focused mainly on the excited-state behavior of the TICT molecules.

The electronic absorption spectrum of anthracene has been a subject of interest to many researchers for several years. A number of papers are published in an attempt to understand the photodynamics of this molecule. Since the early work of Platt[13] and Clar,[14] it has been recognized that the long-wavelength absorption band of anthracene involves two electronic transitions, $^1A \rightarrow {}^1L_a$ and $^1A \rightarrow {}^1L_b$ ($^1A_g \rightarrow {}^1B_{1u}$ and $^1A_g \rightarrow {}^1B_{2u}$, respectively in Mulliken's notations[15]). However, no experimental evidence was available until recently when a two-photon absorption experiment by Wolf et al. indicated the presence of a strong absorption at 29 555 cm^{-1} (338 nm) which has been assigned to the ^1L_b transition.[16] Substitution at various positions of the anthracene ring by electron-donating as well as accepting functional groups failed to resolve these transitions. However, the 9-substituted anthracene derivatives exhibited interesting spectral properties in solution. For example, fluorescence studies of 9- and 10-substituted anthracene derivatives have shown that at high concentrations, these molecules display a new broad emission band on the long-wavelength side of the normal emission. This emission has been ascribed to the excimer formation.[17−20] As mentioned in the preceding paragraph, anomalous fluorescence of ADMA has already been observed. The dual fluorescence of 9-anthracenecarboxylic acid in protic solvents has also been studied extensively.[21−25] Similarly, the absorption spectrum of 9-aminoanthracene (9-AA) showed a broad red-shifted long-wavelength band.[26]

In this work, we present the absorption and fluorescence spectral characteristics and the photophysical properties of 9-(*N*,*N*-dimethylamino)anthracene (9-DMA) in a series of organic solvents and solvent mixtures of varying polarity and viscosity. We also attempt to calculate energies of various conformers obtained by twisting the $-N(CH_3)_2$ group around the C−N bond.

Experimental Section

Materials. The 9-DMA was synthesized by reaction of 9-bromoanthracene with lithium dimethylamide in dry ether under nitrogen atmosphere at room temperature following a standard literature method.[27] The compound was identified by ^1H NMR [$N(CH_3)_2$, 3.24 (s, 6H); Ar−H, 7.4 (m, 4H), 7.9 (m, 2H), 8.3 (m, 3H)] and UV−vis spectra. The compound was purified on a silica column using chloroform as the eluting

* Author to whom correspondence should be addressed.
[⊗] Abstract published in *Advance ACS Abstracts,* June 15, 1997.

S1089-5639(96)03869-8 CCC: $14.00

solvent. The purity was confirmed by the appearance of a single spot on the TLC plate after elution with chloroform. Anhydrous HPLC grade cyclohexane (Aldrich), acetonitrile (Mallincrodt), methanol (A.C.S.), ethanol (EM), tetrahydrofuran (EM), 1,2-dimethoxyethane (Aldrich), dimethylformamide, DMF (Mallincrodt), ethylene glycol (Aldrich), dimethyl sulfoxide, DMSO (Mallincrodt), and glycerol (Aldrich) were used as received. Analytical grade $HClO_4$ (A.C.S.), H_3PO_4 (A.C.S.), NaH_2PO_4, Na_2HPO_4 (Fischer), and NaOH (Becker) were also used as received. The β- and γ-cyclodextrins were obtained from Sigma Chemicals and were used without further purification. Megapore HPLC grade deionized water was used for preparation of aqueous solutions.

Methods. Fluorescence quantum yields (Φ) were estimated by use of Parker's method[28] using quinine bisulfate in 0.1 N H_2SO_4 as the fluorescence standard ($\Phi = 0.545$).[29] All solutions including quinine sulfate were excited at 350 nm.

The measurement of fluorescence lifetimes was performed on a PTI Inc. LS-100 Luminescence Spectrometer with a nitrogen flash lamp as the excitation source. The 337 and 358 nm emissions of nitrogen were used for sample excitation. The decay curves were obtained by use of the time-correlated single photon counting (TC-SPC) method. A total of 2×10^4 counts at the peak channel was collected. Each data set was collected in 512 channels. The data were analyzed by using a multiexponential decay analysis program. The goodness of fit between the measured and calculated decay curves was evaluated by use of the randomness of the weighted residuals and the autocorrelation function and the reduced χ^2 (0.9−1.2) and Durbin−Watson parameters. All measurements were repeated at least twice to verify data reproducibility.

Apparatus. Absorption spectra were recorded using a double-beam Shimadzu UV-3101PC Scanning Spectrophotometer equipped with a constant temperature circulator. Fluorescence spectra were measured on a Spex-Fluorolog model F2T21I spectrofluorometer equipped with a cell compartment thermostated by use of a VWR model 1160 constant temperature circulator. All absorption and fluorescence measurements were conducted at 25 °C. The band-pass of the excitation and emission monochromators was set at 5 and 3.4 nm, respectively. Low-temperature fluorescence and fluorescence polarization spectra were recorded by use of a PTI Inc. LS-100 Luminescence Spectrometer.

The induced circular dichroism spectrum was measured under nitrogen atmosphere on a Jasco J-710 Spectropolarimeter using a cylindrical quartz cuvette of 1 cm path length. For each spectrum, 3−5 scans were accumulated. The ^{1}H NMR spectra of 9-DMA were recorded on a Brucker 250 MHz instrument using TMS as the internal reference.

Results

Absorption Spectra. The electronic absorption spectra of 9-DMA in selected organic solvents are depicted in Figure 1. The absorption spectrum consists of a two-band system, an intense short-wavelength band at ~250 nm and a relatively weak but structured band in the wavelength range of 300−450 nm. The progressions in the long-wavelength band are very similar to that of anthracene, except that the structured band has a broad tail which extends up to 450 nm. In aprotic polar solvents such as acetonitrile, the broad band becomes more pronounced. However, in protic solvents, the intensity of the broad band decreases. Upon acidification, the tail completely disappears (Figure 1) and the spectrum resembles that of the parent hydrocarbon, anthracene. To locate the positions of the ^1L_a and ^1L_b transitions in the absorption spectrum, we have measured

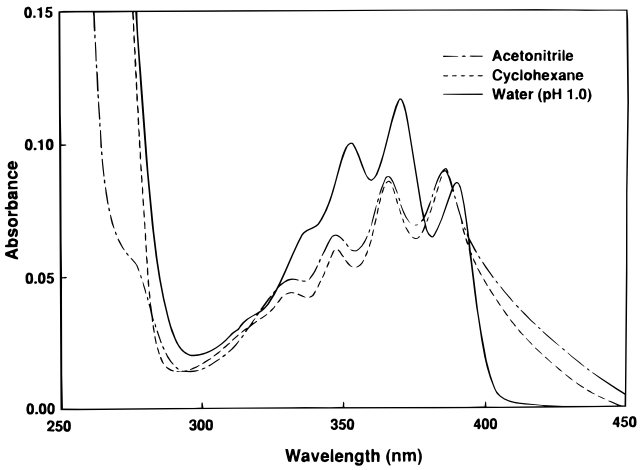

Figure 1. Absorption spectra of 9-DMA in various solvents.

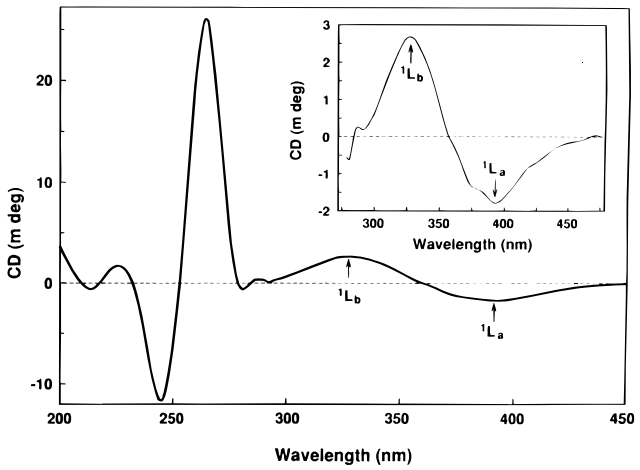

Figure 2. Induced circular dichroic spectrum of 9-DMA in aqueous solution of γ-cyclodextrin; long-wavelength CD bands of 9-DMA (inset).

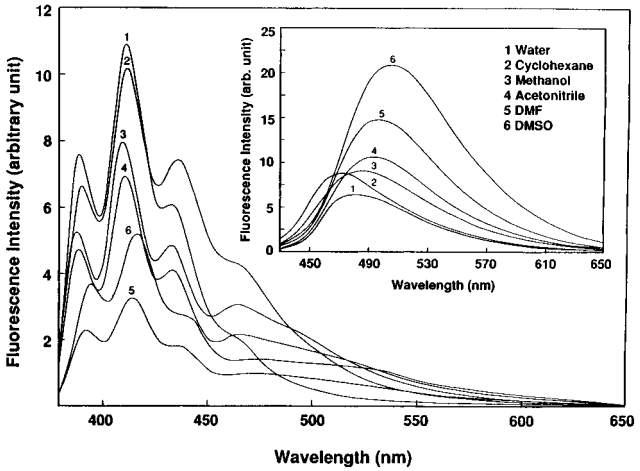

Figure 3. Fluorescence spectra of 9-DMA in different solvents, λ_{ex} = 350 nm; fluorescence spectra at λ_{ex}= 420 nm (inset).

the induced circular dichroic (ICD) spectra of 9-DMA in β- and γ-cyclodextrin. The β-CDx failed to induce significant dichroism in 9-DMA in aqueous solution. However, in the presence of γ-CDx, the molecule exhibits a negative as well as a positive CD band (at 400 and 330 nm, respectively) in the spectral region of the long-wavelength absorption band along with a strong positive signal corresponding to the ^1B_b transition at shorter wavelength (Figure 2).

Fluorescence Spectra. The fluorescence spectra of 9-DMA in selected solvents are portrayed in Figure 3. A summary of

TABLE 1: Absorption and Fluorescence Maxima (λ_{max}(abs) and λ_{max}(flu), Respectively), Fluorescence Quantum Yields (Φ_f), and Fluorescence Lifetimes (τ_f) of 9-DMA in Various Solvents

solvent	λ_{max}(abs) (nm)	λ_{max}(flu)[a] (nm)	Φ_f (±0.001)	τ_f (±0.2 ns)
cyclohexane	386	462 (472)	0.008	4.3, 1.6
	366	436		
	347	412		
	331(s)	391		
	249			
1,4-dioxane	387	466 (478)	0.013	5.8, 0.9
	366	434		
	349	414		
	333(s)	392		
	250			
1,2-dimethoxyethane	386	468 (486)	0.007	4.8, 1.9
	366	434		
	348	413		
	333(s)	392		
	249			
tetrahydrofuran	386	466 (482)	0.010	5.3, 1.3
	366	434		
	348	414		
	332(s)	392		
	250			
acetonitrile	386	466 (494)	0.007	3.9, 1.3
	366	434		
	347	412		
	332(s)	390		
	248			
dimethylformamide	388	470 (492)	0.016	6.5, 1.3
	368	434		
	349	415		
	332(s)	392		
dimethyl sulfoxide	390	472 (506)	0.018	8.2, 0.9
	370	436		
	350	417		
	334(s)	395		
	260			
ethanol	385	464 (484)	0.007	5.1, 1.3
	365	433		
	347	410		
	330(s)	389		
	248			
methanol	384	464 (485)	0.008	4.0, 1.6
	365	432		
	346	410		
	330(s)	389		
	248			
ethylene glycol	388	474 (488)	0.022	7.0, 0.7
	368	436		
	349	414		
	256	392		
glycerol	393	483 (498)	0.068	8.9, 1.8
	373	442		
	354	415		
	335	393		
water (20% ethanol, pH 7.2)	385	460 (480)	0.011	5.7, 1.3
	365	434		
	345	412		
	249	390		
water (cation, pH 1.0)	389	475(s)	0.520	17.3
	370	440(s)		
	353	422		
	343(s)	400		
	253			

[a] (s), shoulder. [b] The wavelength within the parentheses is the emission maximum at λ_{ex} = 420 nm.

the emission maxima and the photophysical properties appear in Table 1. The most interesting feature of the fluorescence spectrum of 9-DMA is that it exhibits dual emission bands in all solvents employed in this study. The normal Stokes-shifted emission (F_n) band is vibronically resolved and resembles the structured fluorescence spectrum of anthracene. However, the large Stokes-shifted emission (F_a) band is structureless and weaker in intensity as compared to the normal band. In fact, the long-wavelength (LW) emission in nonpolar solvents, e.g., cyclohexane, appears as a shoulder to the short-wavelength (SW) band. As the solvent polarity increases, the F_a emission becomes more prominent. However, in protic solvents such as alcohol and water, the intensity of the band decreases and merges with the SW band. Upon acidification, the F_a emission completely disappears . The spectra in Figure 4 show that the fluorescence intensity of the SW band of 9-DMA in aqueous solution increases with a decrease in pH. In viscous solvents, e.g., in glycerol, the emission bands are of comparable to each other in intensity. To examine the effect of viscosity, we have measured the fluorescence spectra of 9-DMA in ethanol containing varying percentages of glycerol. The spectra in Figure 5 clearly show that the intensity of the F_a emission increases as the percentage of glycerol increases. Although the intensity of both bands increases with an increase in viscosity, the increase in intensity of the LW band is higher than that of the SW band. The ratio (I_a/I_n) of the intensities of the F_a and F_n emissions at the respective emission maximum are plotted in Figure 5 (inset) against the percentage of glycerol. Clearly, the ratio increases with an increase in viscosity of the medium.

We have also measured the fluorescence spectrum of 9-DMA in ethanol at 77 K (Figure 6). As noted, the intensity of the LW band is much higher when compared to the intensity of the SW band. Also, the LW emission is structured and is blue

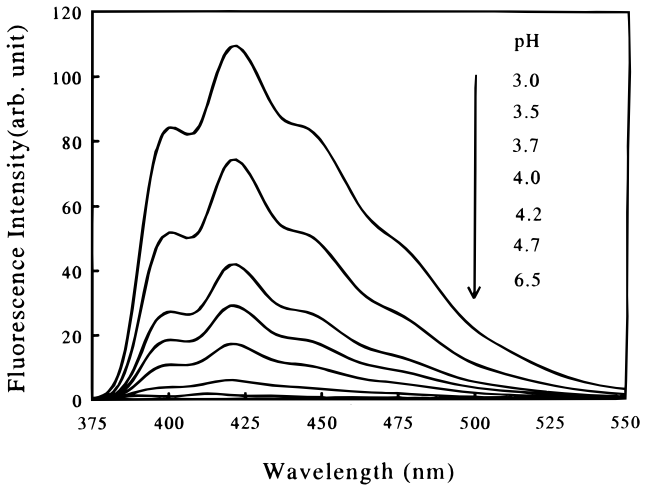

Figure 4. Fluorescence spectra of 9-DMA in aqueous solutions at various pHs.

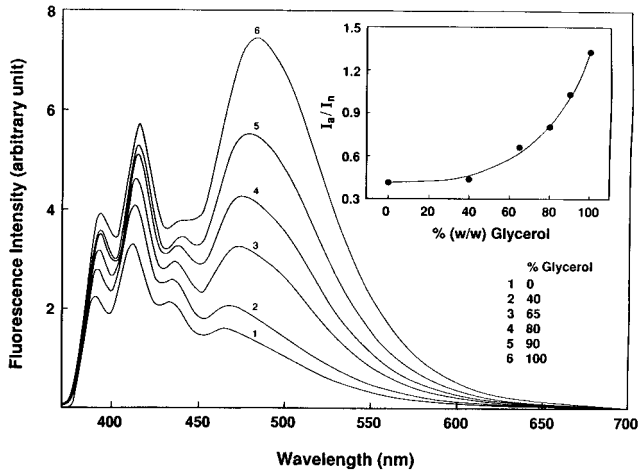

Figure 5. Fluorescence spectra of 9-DMA in ethanol−glycerol mixtures of varying composition, λ_{ex} = 360; plot of intensity ratio (I_a/I_n) vs % (w/w) of glycerol (inset).

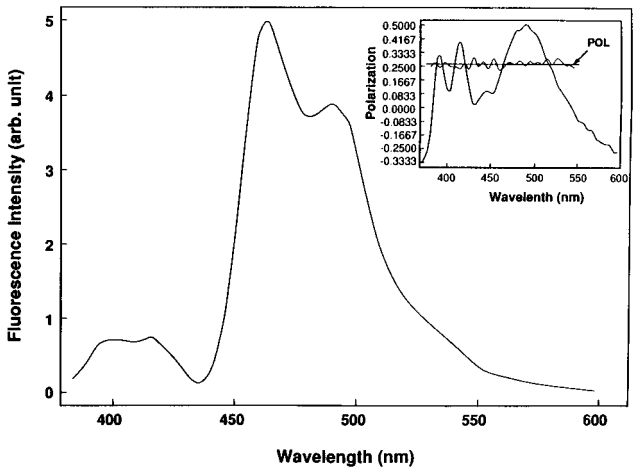

Figure 6. Fluorescence spectrum of 9-DMA in ethanol glass (77 K); fluorescence and fluorescence polarization spectra of 9-DMA in glycerol at 272 K (inset).

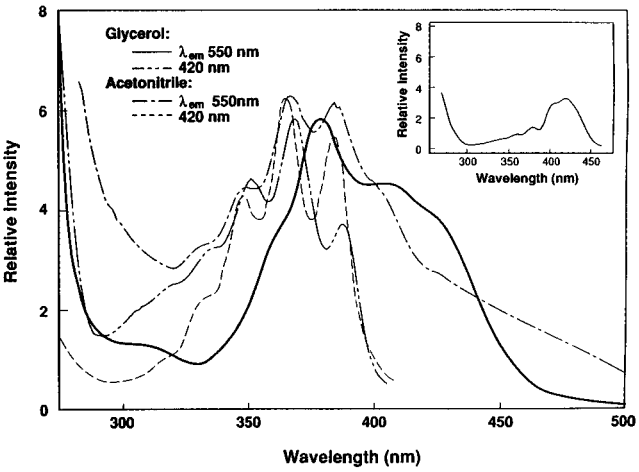

Figure 7. Fluorescence excitation spectra of 9-DMA in acetonitrile and glycerol; fluorescence excitation spectrum in ethanol glass (inset).

shifted as compared to that in fluid solvent at room temperature. The intensity ratio (I_a/I_n) of the emission bands, at the respective emission maximum in acetonitrile, does not change significantly upon increase in concentration of the fluorophore over the range of 10^{-6} to 5×10^{-4} M. The fluorescence excitation spectra of the corresponding emission bands observed in acetonitrile are clearly different from each other (Figure 7). The fluorescence excitation spectrum corresponding to an emission wavelength of 550 nm resembles the absorption spectrum. However, the excitation spectrum corresponding to the F_n emission (420 nm) only shows the structured portion of the LW absorption band. The differences in the excitation spectra are clearly evident in glycerol solvent. Figure 7 also shows the fluorescence excitation spectrum of 9-DMA in ethanol at liquid nitrogen temperature (77 K). Clearly, a broad red-shifted band can be seen on the long-wavelength side of the structured absorption band at low temperature. The fluorescence polarization spectrum of 9-DMA (Figure 6 (inset)) in glycerol at 272 K shows identical positive polarization for both emission bands.

Fluorescence Quantum Yields and Lifetimes. The data in Table 1 indicate that the fluorescence quantum yield of 9-DMA decreases as the solvent polarity increases from cyclohexane to acetonitrile. However, in water, the Φ_f value is higher than in methanol, although the polarity of the former solvent is twice as high as that of the latter. It is interesting to note that the Φ_f values are much higher in DMF, DMSO, ethylene glycol, and glycerol. The fluorescence decays in the solvents studied are

TABLE 2: Fluorescence Lifetimes (τ) of 9-DMA in Aqueous Solution Containing Various Percentages of Sucrose

% (w/w) sucrose	viscosity (η/η_0)[a]	τ_1 (±0.1 ns)	τ_2 (±0.2 ns)
14	1.531	7.8	1.2
22	2.12	8.3	1.4
26	2.568	8.4	1.3
30	3.181	8.7	1.3
40	6.15	8.8	0.9
44	8.579	9	1.6
50	15.4	9.2	1.2
54	24.63	9.3	2
60	58.37	9.7	2.3

[a] The values are taken from ref 30.

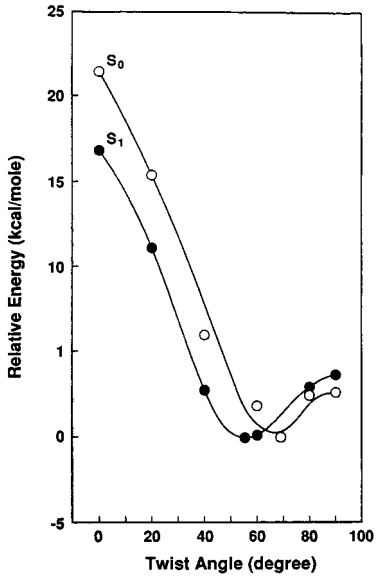

Figure 8. Plot of relative energy vs twist angle (θ) of various conformers of 9-DMA.

emission wavelength-dependent. At emission wavelengths below 415 nm, the fluorescence decay is single exponential corresponding to a single emitting state. However, at higher wavelengths all decays are biexponential. The amplitude of the short-lived and the long-lived component, respectively increases and decreases as the monitored emission wavelength is moved to longer wavelengths. The τ_f value of the long-lived component decreases with an increase in solvent polarity but increases in going from aprotic to protic solvent. It is important to note that the fluorescence decay of the cationic species is single exponential. The τ_f value of the cation is very high as compared to the neutral molecule. This is consistent with the high fluorescence quantum yield of the protonated species. The data in Table 1 show that the fluorescence lifetimes of both long- and short-lived species are higher in viscous solvents such as ethylene glycol and glycerol. To demonstrate the effect of viscosity of the solvent, we have measured the fluorescence lifetime of 9-DMA in aqueous solutions containing various percentages of sucrose. The lifetime data along with the viscosity values[30] are presented in Table 2. It can be seen that the fluorescence lifetime (τ_1) of the long-lived component increases as the viscosity of the medium increases.

Theoretical Calculation. The AM1 calculations[31] were performed to understand the fluorescence spectral behavior of 9-DMA. The unrestricted geometry optimization at the semiempirical level was carried out for various twist angles of the $-N(CH_3)_2$ group around the C−N bond. In Figure 8, we have presented the variation of the ground (S_0) and excited (S_1) state energies as a function of the twist angle (θ) of the $-N(CH_3)_2$ group. The plots suggest that in the ground state equilibrium

geometry the $-N(CH_3)_2$ group is twisted at an angle of 69°. This result is close to that in *N*,*N*-2,6-tetramethylaniline (68°).[32] However, in the case of *N*,*N*-dimethylaniline, the nitrogen center is close to trigonal ($\theta \sim 0°$) in the vapor phase.[33] In the S_1 state, the $-N(CH_3)_2$ group becomes more planar as suggested by the twist angle (56°). The decrease of twist angle is accompanied by a decrease in C−N bond length (from 1.432 to 1.395 Å) and an increase in dipole moment (from 0.77 to 2.22 D) of the molecule in going from the S_0 to S_1 state. Further, the energy barrier between the equilibrium geometry ($\theta = 69°$) and the fully twisted form ($\theta = 90°$) is found to be small in both the S_0 and S_1 states (2.6 and 3.7 kcal/mol, respectively). However, for the planar conformation ($\theta = 0°$), the calculated energy barrier is much higher (15−22 kcal/mol) in both S_0 and S_1 state.

Discussion

In analogy with anthracene, the strong absorption band at ∼250 nm in the absorption spectrum of 9-DMA can be assigned to ^1B_b transition. The positions of the ^1L_a and ^1L_b transitions in the absorption spectrum are indicated by the ICD spectrum of 9-DMA in Figure 3. The positive CD band corresponding to the ^1B_b transition suggests that the molecule is axially oriented in the γ-CDx cavity since equatorial inclusion of 9-DMA is sterically prohibited. According to the Kirkwood−Tinoco's rule[34] based on double-oscillator coupling theory, the negative band at ∼400 nm and the positive band at ∼330 nm correspond, respectively, to the ^1L_a and ^1L_b transitions. The development of the broad absorption band at the extreme long-wavelength end of the spectrum is a feature common to aromatic amines of this type. This effect can be attributed to a weak interaction between the anthracene and the $-N(CH_3)_2$ group. This leads to the presumption that an extra red-shifted and broad absorption band exists in the case of 9-DMA, which may be attributed to a direct transition to a CT state. This tentative assignment is based on the observation that at low pH (1.0) the broad tail of the absorption spectrum disappears (Figure 1) when the amino group is protonated and the spectrum becomes nearly the same as that of anthracene. Such spectral behavior has also been reported for 9-AA.[26] It is expected that the absorption spectrum of 9-DMA should be similar to that of 9-AA in the same solvent. In contrast, as reported in the literature, the long-wavelength absorption band of the latter molecule is more pronounced and red-shifted as compared to that of 9-DMA.[26] This suggests that the electronic interaction between the unsubstituted amino group and the aromatic ring is stronger in 9-AA than that between the $-N(CH_3)_2$ group and the aromatic ring in 9-DMA. This is indicated by the pK_a values of the respective ammonium ions of 9-AA (2.7)[35] and 9-DMA (3.8). The difference (1.1) between the pK_a values of 9-AA and 9-DMA is greater than that between aniline (4.6)[36] and *N*,*N*-dimethylaniline (5.06).[37] This is likely due to the steric hindrance of the *peri*-hydrogens at positions 1 and 8 of the aromatic ring which prevents free rotation of the $-N(CH_3)_2$ group around the C−N bond, thus causing the lone-pair-electron orbital to be out of plane of the p-orbitals of the aromatic ring. Consequently, electronic interaction of the group with the aromatic ring may be weaker. This is further supported by the calculated twist angle (69°) of the plane containing the $-N(CH_3)_2$ group with respect to the aromatic ring.

The resemblance of the structured fluorescence band of 9-DMA with that of anthracene suggests that the SW emission originates from the local excited (LE) state. As noted before, the large Stokes-shifted fluorescence can result from a variety of phenomena. Since the ratio of the intensities of the long and short-wavelength bands remained unaltered when excited at different wavelengths in the range of 300−400 nm, and also the time-resolved fluorescence of the protonated species resulted in a single exponential decay, fluorescence due to impurities in the sample is not likely. The concentration independence of the intensity ratio (I_a/I_n) also rules out the possibility of any excimer fluorescence. The fluorescence due to formation of a hydrogen-bonded complex in a polar protic solvent can be ruled out on the basis of the fact that the long-wavelength fluorescence band is also observed in aprotic polar solvents, e.g., acetonitrile.

The solvent and the pH dependence of the fluorescence intensity of the emission bands clearly suggest that the LW emission is CT type. The fluorescence from a CT state is usually weak because of a low S−T energy gap which enhances the intersystem crossing rate. Since the CT state is more stable in polar solvents, the Φ_f value for CT emission should decrease with an increase in solvent polarity. However, in protic solvents (e.g., water), the intermolecular hydrogen bonding of the amino group with the solvent molecules reduces the CT character of the emitting state. Consequently, the fluorescence quantum yield of 9-DMA is higher in water than in less polar solvents. The effect of hydrogen bonding on the fluorescence quantum yield is demonstrated by the Φ_f and τ_f value of the cationic species. Since protonation is the extreme case of hydrogen bonding, it totally destroys the charge-transfer interaction of the lone-pair-electrons of the amine group with the p-electrons of the aromatic ring, thus decreasing the nonradiative decay rates. This results in an increase in fluorescence from the LE state. The increase of Φ_f and τ_f value in viscous solvents is also due to decrease in nonradiative deactivational rates.

The F_a emission could be attributed to a TICT state emission as observed for example, in the case of DMABN.[1−6] A TICT state contains two separated charged moieties within a molecule, geometrically disposed to assure a minimum overlap of their orbitals and involves a rather large change in dipole moment.[8,38] The emission from such a polar state occurs at a much longer wavelength and is strongly dependent on the solvent polarity.[8] In the case of 9-DMA, the wavelength shift between cyclohexane and acetonitrile corresponds to a small energy difference (943 cm^{-1}), which is incompatible with an emission originating from a TICT-type species. The results of theoretical calculation also indicate a small increase in dipole moment of the molecule upon electronic excitation. Moreover, the TICT state formation involves a rotation of the $-N(R)_2$ group around the C−N bond in the excited state. Such rotation is not favored in viscous solvents. Therefore, the fluorescence intensity of the TICT fluorescence should decrease with an increase in viscosity of the solvent. In contrast, the fluorescence intensity of the F_a emission of 9-DMA increases with an increase in viscosity of the solvent (Figure 5). Therefore, the large Stoke-shifted emission cannot be associated with the TICT process.

Another possible explanation for the appearance of dual emission would be emission from both ^1L_a and ^1L_b states as originally proposed for DMABN.[1,39] In such a case, one would expect the corresponding fluorescence excitation spectra to be identical. However, since the fluorescence excitation spectra (Figure 7) for the emission bands are different, the possibility of emission from two different excited states can be eliminated. This conclusion is further supported by the fluorescence polarization spectrum in glycerol (Figure 6), which shows that the two emission bands have identical polarizations (∼0.269). It is interesting to note that both emission bands are of comparable intensity in glycerol although the viscous solvent cannot reorient extensively during the lifetime of the excited state. The high degree of polarization is further proof that in glycerol, where both the solvent and solute molecules are of

comparable size, rotational depolarization is negligible. The positive polarization suggests that the transitions involved in the absorption and emission processes are parallel and both the emitting states are of ^1L_a type. This means that the dual fluorescence originates from two ^1L_a states of two different forms of the molecule present in the ground state. The observed excitation energy dependence of 9-DMA fluorescence supports this conclusion. Thus, the observed absorption spectrum of 9-DMA is a superposition of the absorption spectra of two different forms of the same molecule. The appearance of only the F_a emission when excited at wavelengths higher than 410 nm suggests that one of the forms of the molecule is preferentially excited and the measured fluorescence spectra are characteristic of that form. On the short-wavelength side, however, both forms are excited so that the resultant fluorescence spectra are the superposition of the spectra of both forms. The existence of conformational equilibrium at room temperature in both the ground and excited states has been demonstrated by the fluorescence emission and excitation spectra in ethanol glass at 77 K. At room temperature, the intensity of the CT absorption is much weaker compared to the main absorption band. Similarly at room temperature the main fluorescence occurs at short wavelengths. However, at 77 K, the intensities of both CT absorption and emission are higher compared to the absorption and emission at shorter wavelengths.

Thus, at this stage, the SW emission can be attributed to a molecular structure in which the electronic energy levels of anthracene are not significantly perturbed by the $-N(CH_3)_2$ substituent at the 9-position. That is, no significant resonance interaction exists between the $-N(CH_3)_2$ group and the anthracene ring. This can occur when the plane containing the $N-CH_3$ bonds is orthogonal to the anthracene moiety. Thus, the absorption and fluorescence spectra of this conformer (I) are expected to be similar to that of anthracene. If a TICT state was developing with this appropriate structure, one would expect a decrease in the F_a emission when the temperature is lowered to 77 K. Since this is definitely not the case, one cannot attribute the long-wavelength emission to a TICT state. In the other conformer (II), the $-N(CH_3)_2$ group is partially twisted ($\theta = 56°$) with respect to the plane of the aromatic ring. From first-order perturbation theory, the resonance energy is approximately proportional to $\cos^2\theta$, where θ is the twist angle.[40] Therefore, at $\theta = 56°$, almost one-half of the maximum resonance energy would be expected. This implies that complete coplanarity between the $-N(CH_3)_2$ and the ring is not essential for a significant resonance interaction to occur.

The assumption that two conformers are present in the ground as well as in the excited state is also supported by the results of the AM1 calculations. Since the available thermal energy at room temperature is comparable to the energy barrier associated with the twisting process, one can expect the fully twisted form (I) to be present in significant concentrations at room temperature and contribute to both absorption and emission processes in fluid solvents. However, in viscous and glassified solvents, this energy barrier is expected to be higher and therefore contributions due to the fully twisted form will be less. This explains the decrease and increase in fluorescence intensity of the SW and LW emission bands, respectively, in ethanol glass at 77 K as discussed previously. This suggests that the long-wavelength emission is associated with the partially twisted conformer (II) and the normal emission with a fully twisted conformer (I) of the molecule. The existence of ground-state equilibrium between conformers of 4-cyano-1-(*N*,*N*-dimethylamino)naphthalene has also been proposed.[41]

Conclusions

It has been demonstrated that the absorption spectrum of 9-DMA is a superposition of the spectra of two conformers. In conformer I, the -$N(CH_3)_2$ group is estimated by AM1 calculation to be fully twisted ($\theta = 90°$), whereas in conformer II, AM1 calulations predict an angle of 69° in the S_0 state and 56° in the S_1 state. The long wavelength transitions of both conformers are ^1L_a type. In the case of conformer, I, the ^1L_a transition is p → p* type whereas in conformer II, it is charge transfer in nature and is red-shifted relative to that of I. The induced circular dichroic spectra of 9-DMA have indicated the position of ^1L_b transition at around 330 nm in the absorption spectrum. The dual fluorescence originates from the ^1L_a states of both conformers. The large Stokes-shifted CT type fluorescence is associated with conformer II, and the normal Stokes-shifted fluorescence with conformer I. The viscosity dependence of the fluorescence quantum yield and lifetime of the molecule makes it a good fluorescence probe for studies of microenvironments of organized media.

Acknowledgment. The authors acknowledge the Department of Energy (DE-FG05-93ER-14367) and National Science Foundation (CHE 9224177) for partial support of this research. The authors are also thankful to Dr. Asit K. Chandra for his assistance with the theoretical calculations. I.M.W. acknowledges the Phillip W. West endowment for partial support of this research.

References and Notes

(1) Lippert, E.; Luder, W.; Boos, H. In *Advances in Molecular Spectroscopy*; Mangini, A., Ed.; Pergamon Press: New York, 1962; p 443.
(2) Rotkiewicz, K.; Grellmann, K. H.; Grabowski, Z. R. *Chem. Phys. Lett*. **1973**, *19*, 315.
(3) Grabowski, Z. R.; Rotkiewicz, K.; Siemiarczuk, A.; Cowley, D. J.; Baumann, W. *Nouv. J. Chim*. **1979**, *3*, 443.
(4) Lippert, E.; Rettig, W.; Bonacic-Koutecky, V.; Heisel, F.; Mieche, J. A. In *Advances in Chemical Physics*; Prigogine, I., Rice, S. A., Eds.; Wiley-Interscience: New York, 1987; Vol. 68, pp 1−173.
(5) Weller, A. *Z. Elektrochem*. **1956**, *60*, 1144.
(6) Kasha, M. *J. Chem. Soc., Faraday Trans*. **1986**, *82*, 2379.
(7) Bonacic-Koutecky, V.; Bruckman, P.; Hiberty, P.; Koukecky, J.; Leforestier, C.; Salem, L. *Angew. Chem*. **1975**, *87*, 599.
(8) Rettig, W. *Angew Chem., Int. Ed. Engl*. **1986**, *25*, 971.
(9) (a) Schneider, F.; Lippert, E. *Ber. Bunsen-Ges. Phys. Chem*. **1968**, *72*, 1155. (b) Schneider, F.; Lippert, E. *Ber. Bunsen-Ges. Phys. Chem*. **1970**, *74*, 624. (c) Beens, H.; Weller, H. *Chem. Phys. Lett*. **1969**, *3*, 666. (d) Rettig, W.; Zander, M. *Ber. Bunsen-Ges. Phys. Chem*.**1983**, *87*, 1143. (e) Yamasaki, K.; Arita, K.; Kajimoto, O.; Hara, K. *Chem. Phys. Lett*. **1986**, *123*, 277.
(10) (a) Wiessner, A.; Huttmann, G.; Kuhnle, W.; Staerk, H. *J. Phys. Chem*. **1995**, *99*, 14923. (b) Okada, T.; Mataga, N.; Baumann, W.; Siemiarczuk, A. *J. Phys. Chem*. **1987**, *91*, 4490.
(11) Dey, J.; Dogra, S. K. *J. Phys. Chem*. **1994**, *98*, 3638.
(12) Rotkiewicz, K.; Rubaszewska, W. *J. Lumin*. **1982**, *27*, 221.
(13) Platt, J. R. *J. Chem. Phys*. **1949**, *17*, 484.
(14) Clar, E. *Spectrochim. Acta* **1950**, *4*, 116.
(15) Mulliken, R. S. *J. Chem. Phys*. **1955**, *23*, 1997.
(16) Wolf, J.; Hohlneicher, G. *Chem. Phys*. **1994**, *181*, 185.
(17) Vember, T. M.; Cherkasov, A. S. *Opt. Spektrosk.* **1959**, *6*, 232; *Opt. Spectrosc.* **1959**, *6*, 148.
(18) Trischenco, G. A.; Sveshnikov, B. Ya; Cherkasov, A. S. *Opt. Spektrosk.* **1958**, *4*, 631.
(19) Birks, J. B.; Aladekomo, J. B. *Photochem. Photobiol*. **1963**, *2*, 416.
(20) Forster, Th.; Kasper, K. *Z. Phys. Chem*. **1954**, *1*, 275; *Z. Elektrochem*. **1955**, *59*, 976.
(21) Bazilevskaya, N. S.; Cherkasov, A. S. *Opt. Spectrosc*. **1965**, *18*, 30.
(22) Bazilevskaya, N. S.; Cherkasov, A. S. *Zh. Prikl. Spektrosk. Akad. Nauk Belorussk. SSR* **1965**, 548.
(23) Walker, M. S.; Bednar, T. W.; Lumry, R. *J. Chem. Phys*. **1967**, *47*, 1020.
(24) Werner, T. C.; Hercules, D. M. *J. Phys. Chem*. **1969**, *73*, 2005; **1970**, *74*, 1030.
(25) (a) Agbaria, R. A.; Butterfield, M. T.; Warner, I. M. *J. Phys. Chem*. **1996**, *100*, 17133. (b) Dey, J.; Haynes, J. L., III; Chandra, A. K.; Warner, I. M. *J. Phys. Chem*., in press.

(26) (a) Etienne, A.; Rutimeyer, B. *Bull. Soc. Chim. Fr.* **1956**, 1588. (b) Craig, D. P.; Short, L. N. *J. Chem. Soc.* **1945**, 419.
(27) Wittig, G.; Closs, G.; Mindermann, F. *Liebigs Ann. Chem.* **1955**, *594*, 88.
(28) Parker, C. A. *Photoluminescence in Solutions*; Elsevier: Amsterdam, 1968; p 262.
(29) (a) Melhuish, W. H. *J. Phys. Chem.* **1961**, *65*, 229. (b) Meach, S. R.; Phillips, D. *J. Photochem.* **1983**, *23*, 193.
(30) *Handbook of Chemistry and Physics*, 64th ed.; Weast, R. C., Astle, M. J., Beyer, W. H., Eds.; CRC Press Inc.: Boca Raton, FL, 1983.
(31) (a) Dewar, M. J. S.; Dieter, K. M. *J. Am. Chem. Soc.* **1986**, *108*, 8075. (b) Dewar, M. J. S.; Zoebich, F. G.; Healy, E. F.; Stewart, J. J. P. *J. Am. Chem. Soc.* **1985**, *107*, 3902.
(32) Wepster, P. M. In *Progress in Stereochemistry*; Klyne, W., De La Mare, P. B. D., Eds.; Butterworths: London, 1958.
(33) Vilkov, L. V.; Timasheva, T. P. *Dokl. Akad. Nauk SSSR* **1965**, *161*, 351.
(34) Tinoco, I., Jr. *Adv. Chem. Phys.* **1962**, *4*, 113. Kirkwood, J. P. *J. Chem. Phys.* **1937**, *5*, 479.
(35) Ireland, J. F.; Wyatt, P. A. H. *Adv. Phys. Org. Chem.* **1976**, *12*, 131.
(36) Scudder, P. H. *Electron Flow in Organic Chemistry*; John Wiley & Sons, Inc.: New York, 1992; p 262.
(37) Baddeley, G.; Chadwick, J.; Taylor, H. T. *J. Chem. Soc.* **1956**, 451.
(38) Rettig, W. *J. Mol. Struct.* **1982**, *84*, 303. Lippert, E. *Z. Naturforsch.* **1955**, *10a*, 541.
(39) No reference 39.
(40) Jaffe, H. H.; Orchin, M. *Theory and Applications of Ultraviolet Spectroscopy*; John Wiley & Sons Inc. : New York, 1964; p 389.
(41) Ayuk, A. A. *J. Mol. Struct.* **1982**, *84*, 169.